47th AIAA Aerospace Sciences Meeting Including The New Horizons Forum and Aerospace Exposition
5 - 8 January 2009, Orlando, Florida

AIAA 2009-1508

AIAA-2009-1508

47th AIAA Aerospace Science Meeting and Exhibit, Jan. 5-8, Orlando, Florida

A dynamic characteristic filter for DNS/LES of compressible turbulent flows

Noma Park* and Krishnan Mahesh†

University of Minnesota, Minneapolis, MN, 55455, USA

We propose a novel shock-capturing method that is based on the ideas of characteristic filters and dynamic suboptimal control. A cost function is based on the smoothness of the solution, and formally minimized to obtain the unknown coefficient in the shock-capturing numerical fluxes. The proposed dynamic procedure is applied to one–dimensional Euler equation equation and two–dimensional Navier–Stokes equation. The proposed dynamic filter achieved noticeable success in capturing shock while minimizing the overall impact on the solution.

I. Introduction

Non-dissipative discretization schemes are highly desirable for large eddy simulation (LES), but the absence of numerical dissipation in these schemes introduces an issue regarding shock–capturing for compressible flows. Since there is no built-in dissipation, an external discontinuity–capturing scheme should be provided in the form of an artificial dissipation or a filter. The main requirement for such a shock–capturing scheme is to concentrate numerical dissipation only in the vicinity of the flow discontinuity so that unnecessary dissipation is minimized.

Among some possible candidates, we consider the characteristic–based filter due to Yee *et al.*,[10] whose main advantage is that it is implemented as an additional corrector–like step, and that it can be incorporated with any non-dissipative schemes. For example, the filter is successfully applied to unstructured finite-volume scheme[6] and the spectral method.[3] The only issue is that the filter has an adjustable coefficient κ, which is highly problem dependent. Thus, several independent simulations should be performed to find its optimal value. However, the optimality of chosen κ that yields seemingly the best solution at a given instant, becomes suspect for complex unsteady flows where the optimal κ is in general the function of space and time.

The present study deals with a dynamic mechanism to determine such an optimal parameter. If one could quantify "the oscillation near the shock", our goal is to find κ that minimize this quantity. Therefore, searching for such κ is the posed as an optimal control problem. The proposed dynamic procedure is applied to one–dimensional Euler equation solver and two–dimensional Navier–Stokes solver, and its performance and efficiency are discussed.

II. Characteristic-based filter

Flux vector $\mathbf{F}(\mathbf{Q})$ at the cell face f using Roe's approximate Riemann solver takes the form

$$\mathbf{F}_f = \frac{1}{2}\left(\mathbf{F}_{icv1} + \mathbf{F}_{icv2} + \mathbf{R}_f \mathbf{\Phi}_f\right), \tag{1}$$

where $icv1$ and $icv2$ denote two cell center values which share the face f. $\mathbf{R}$ is the right Eigenvector matrix and $\mathbf{\Phi}$ is the vector whose dimension is $\mathbf{\Lambda R}^{-1}\mathbf{\Delta Q}$. Even if one uses non-dissipative differencing schemes, the shock capturing nature of (1) can be preserved by introducing the filter numerical flux:[10]

$$\mathbf{F}^*_f = \frac{1}{2}\mathbf{R}_f \mathbf{\Phi}^*_f. \tag{2}$$

*Postdoctoral research associate, Aerospace Engineering & Mechanics

†Associate Professor, Aerospace Engineering & Mechanics, AIAA member

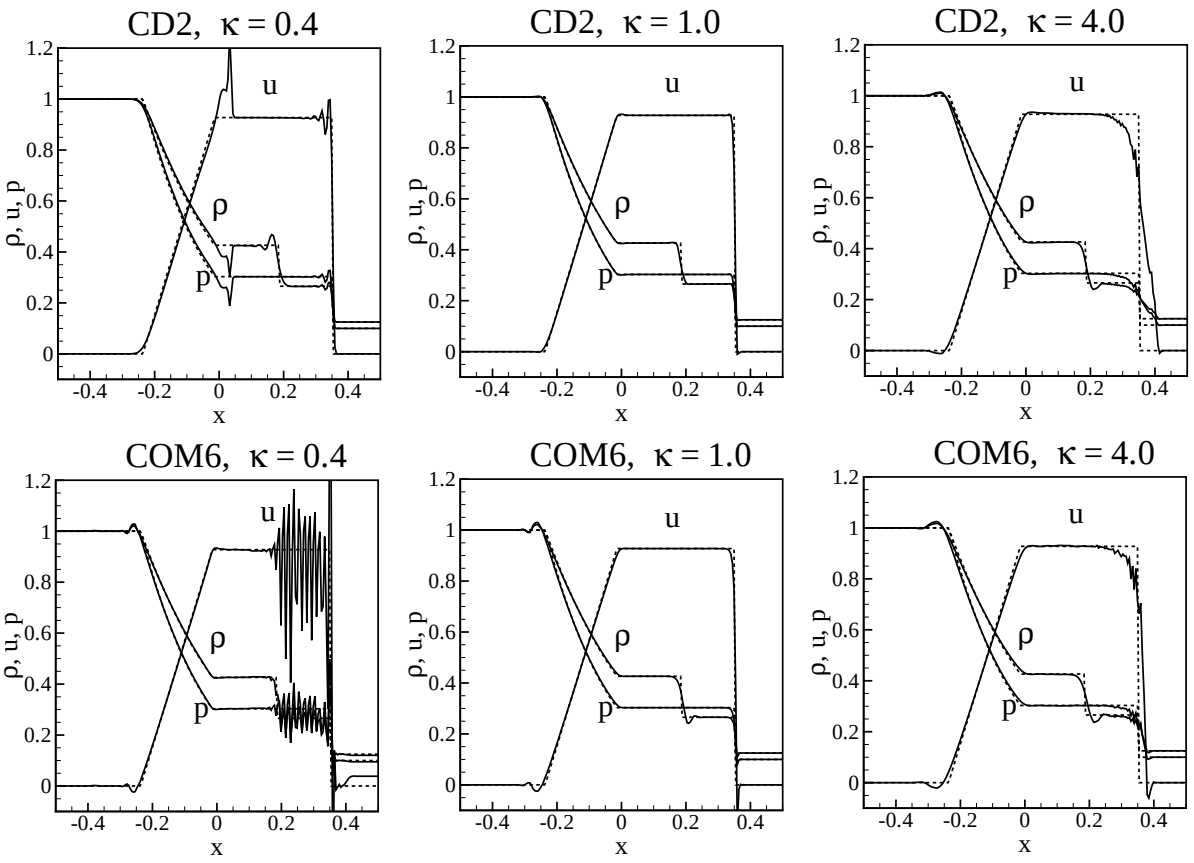

Figure 1. Solutions of the Sod problem at $t = 0.2$ (solid lines) compaerd with the exact Riemann solution (dotted lines) with various values of κ and base discretization schemes. Here, CD2 and COM6, respectively, denote second order central difference and sixth order compact difference schemes.

Once a physical time step Δt is advanced to get the solution $\hat{\mathbf{Q}}^{n+1}$ from $\mathbf{Q}^n$, the final solution $\mathbf{Q}^{n+1}$ at $t + \Delta t$ is determined from a corrector-like scheme:

$$\mathbf{Q}^{n+1} = \hat{\mathbf{Q}}^{n+1} - \nabla \cdot \mathbf{F}^*_f, \tag{3}$$

The expression for the ℓ-th component of $\mathbf{\Phi}^*$, $\phi^{*\ell}$ is given by

$$\phi^{*\ell}_f = \kappa \theta^\ell_H \theta_D \phi^\ell_f, \tag{4}$$

where κ is the adjustable parameter, θ^ℓ_H is the Harten switch function and ϕ^ℓ is the Harten-Yee TVD form. See Yee *et al.* (1999) for details. θ_D is an additional switch introduced in Park & Mahesh,[6] which takes the form[2]

$$\theta_D = \frac{(\nabla \cdot \mathbf{u})^2_f}{(\nabla \cdot \mathbf{u})^2_f + \Omega^2_f + \epsilon}, \tag{5}$$

where Ω is the vorticity magnitude and, $\epsilon = 10^{-7}$ is a small positive value. It is shown that a composite switch $\theta^\ell_H \theta_D$ performs well keeping resolved turbulence without changing good shock-capturing capability of the characteristic based filter.[6]

The sensitivity of the solution to κ is illustrated in Fig. 1, where the solutions of the Sod problem are compared with the exact Riemann solution with $\kappa = 0.4$, 1, 4 and two difference discretization schemes, or second order central difference (CD2) and sixth-order compact difference scheme (denoted as COM6). It is shown that $\kappa = 1$ yields the best solution for both schemes, and smaller/larger values result in oscillatory/dissipative results. For CD2, it is readily expected because $\kappa = 1$ corresponds to the Roe's approximate Riemann solver, Eq. (1), if switches are ignored. However, it is not the case with COM6 where the flux

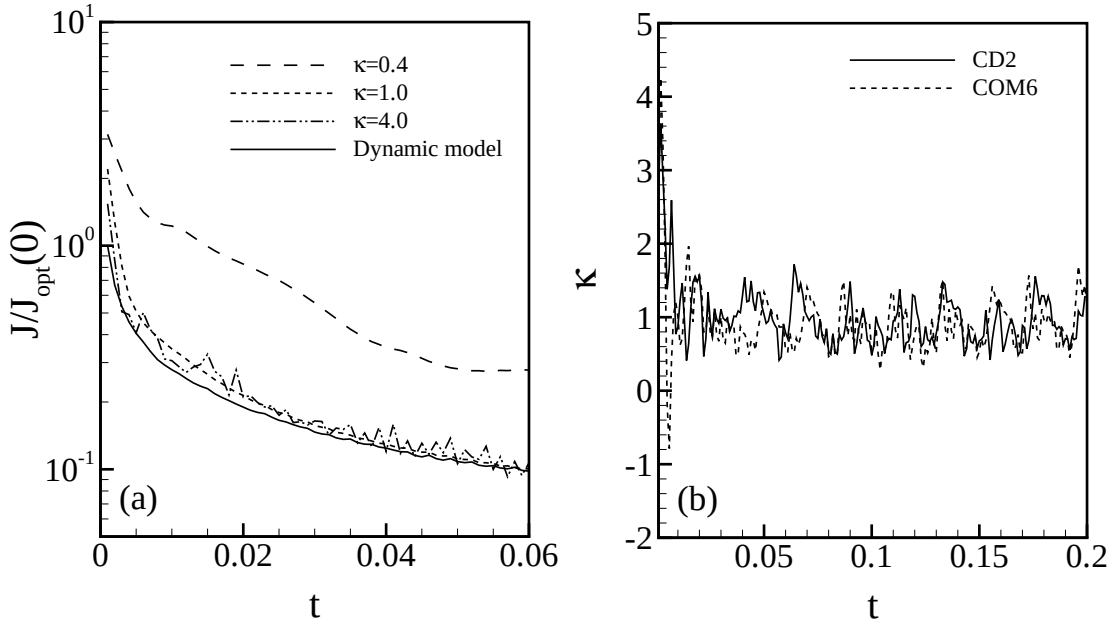

Figure 2. Temporal evolutions of (a) the cost functions from the Euler solver of the Sod problem with CD2, and (b) κ from dynamic model with CD2 and COM6. In (a), cost functions are normalized by the initial cost function value from dynamic model.

at face cannot be defined in a explicit manner. The wiggles shown in the case of $\kappa = 1$ with COM6, may be due to this incompatibility. Numerical experiments show that there is no constant κ that removes these wiggles for COM6. Furthermore, numerical experiments with shock tube problem showed that the optimal κ should be higher as Mach number increases, regardless of discretization scheme. Therefore, an efficient dynamic procedure is required to determine the optimal κ without trial and error.

III. Dynamic procedure for κ

We seek a κ that minimizes the cost function

$$\mathcal{J} = \int_V \theta_D \cdot IS(q)\, dV + \alpha \int_V \kappa^2 dV, \tag{6}$$

where V is the computational domain, θ_D is the divergence–based sensor defined in Eq. (5), and IS is a smoothness indicator for an arbitrary variable q

$$IS(q) = \frac{1}{q_{ref}^2} \sum_{1 \le |\alpha| \le k} \int_\Delta \Delta^{|\alpha|-1} \left(D^\alpha q\right)^2 dV, \tag{7}$$

where q_{ref} is the reference value. Δ is the cell volume, α is the multi index, and D is the derivative operator. The evaluation of $D^\alpha q$ is done by a simple compact finite–difference, instead of exact derivatives of polynomials as in Jiang & Shu.[4] For a two-dimensional flow with $k = 2$, the smoothness indicator is given by

$$IS = \int_\Delta \left[\left(\frac{\partial q}{\partial x}\right)^2 + \left(\frac{\partial q}{\partial y}\right)^2 \right] dxdy + \int_\Delta \Delta \left[\left(\frac{\partial^2 q}{\partial x^2}\right)^2 + \left(\frac{\partial^2 q}{\partial y^2}\right)^2 + \left(\frac{\partial^2 q}{\partial x \partial y}\right)^2 \right] dxdy \tag{8}$$

The second term of Eq. (6), or the price term with a free parameter α, is proportional to the amplitude of solution increment due to filtering. It is necessary to prevent unbounded growth (or decay) of κ. In order to minimize the impact of the shock-capturing method on the solution, α should be as large as possible. The effect of α will be investigated later. Therefore, the minimization of $\mathcal{J}$ can be formally interpreted as the

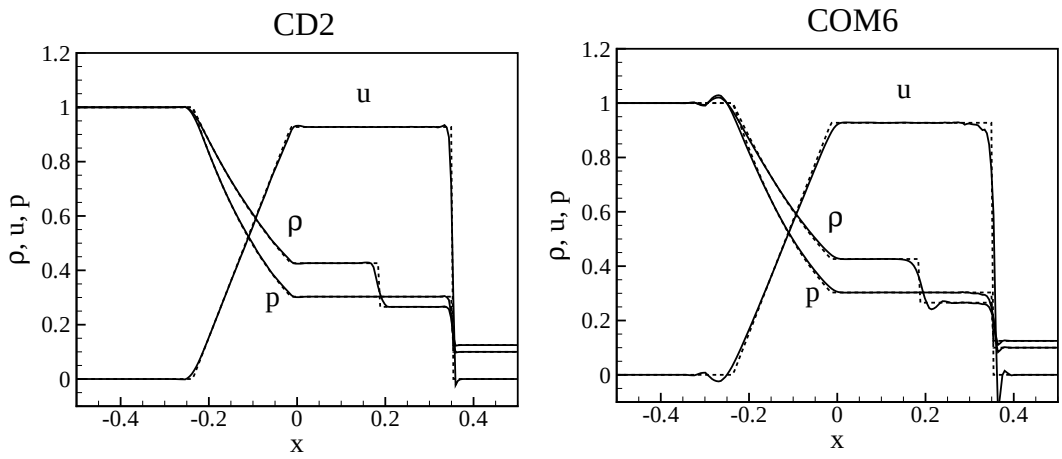

Figure 3. Solutions of the Sod problem at $t = 0.2$ from the global dynamic model. Solid lines are numerical solutions and dotted lines denote the exact Riemann solution.

minimization of the oscillation in the vicinity of the shock, while its impact on the solution is also minimized. In this study, density is chosen for q in the cost function and the smoothness indicator. Temperature or pressure could be used as well, and computational results showed almost identical results.

The cost function minimizer κ can be computed by a gradient–based iteration. The derivative of the cost function in general requires the solution to the adjoint equation,[1] whose computational cost is comparable to the Navier–Stokes solver at each iteration. Thus, total CPU time taken could be 10 to 20 times of the uncontrolled simulation.[5] We therefore use a more efficient approach and directly evaluate the local Fréchet derivatives of the cost function by a method similar to that used in Nicoud *et al.*[5] and Park & Mahesh:[7] Given solution field Q^n and $\hat{Q}^{n+1}$, choose a small ϵ to perturb κ at one point by ϵ and obtain $\kappa + \epsilon\tilde{\kappa}$, where $\tilde{\kappa}$ is a delta function at the location of the perturbation. Now advance velocity field one 'corrector' time step using Eq. (3) and insert this together with $\kappa + \epsilon\tilde{\phi}$ Eq. (6) and (7), and get $\mathcal{J}(\kappa + \epsilon\tilde{\kappa})$. The approximate Fréchet derivative at the location of perturbation is then

$$\frac{\mathcal{D}\mathcal{J}}{\mathcal{D}\kappa}\tilde{\kappa} \approx \frac{\mathcal{J}(\kappa + \epsilon\tilde{\kappa}) - \mathcal{J}(\kappa)}{\epsilon}. \tag{9}$$

Having $\mathcal{D}\mathcal{J}/\mathcal{D}\kappa$ at all points, κ is obtained iteratively by the Pletcher–Reeves conjugate gradient method:[8]

$$\kappa^{k+1}(\mathbf{x}) = \kappa^k(\mathbf{x}) - \lambda^k \mathbf{g}^k(\mathbf{x}), \tag{10}$$

$$\mathbf{g}^k(\mathbf{x}) = \frac{\mathcal{D}\mathcal{J}^k}{\mathcal{D}\kappa} - \frac{\left(\frac{\mathcal{D}\mathcal{J}}{\mathcal{D}\kappa}^k \cdot \frac{\mathcal{D}\mathcal{J}}{\mathcal{D}\kappa}^k\right)}{\left(\frac{\mathcal{D}\mathcal{J}}{\mathcal{D}\kappa}^{k-1} \cdot \frac{\mathcal{D}\mathcal{J}}{\mathcal{D}\kappa}^{k-1}\right)}\mathbf{g}^{k-1}(\mathbf{x}), \tag{11}$$

where $\mathbf{g}^0 = \mathcal{D}\mathcal{J}^0/\mathcal{D}\delta\kappa$, $(\phi \cdot \psi) = \int_\Omega \phi(\mathbf{x})\psi(\mathbf{x})d\mathbf{x}$ is the inner product between two vectors. At each time step, sub-iteration (10) starts with $\kappa^0 = 0$. The constant λ^k is chosen to minimize the cost function by the line–minimization algorithm.[1] Finally, the converged κ is inserted to Eq. (3) to finish the time integration. Numerical tests showed that the proposed optimization is approximately five to ten times faster than adjoint based approach.

IV. Numerical tests

The proposed dynamic characteristic filter (denoted as DCF hereinafter) is first applied to the Sod problem mentioned above, assuming constant κ in space. As shown in Fig. 2, DCF shows smaller cost function that those with constant κ. The computed optimal κ is highly oscillatory in time, but the averaged values approach 1, the known optimal value from Fig. 1. This validates the proposed DCF. As a consequence, the solutions from DCF are similar to those from constant $\kappa = 1$ (Fig. 3).

Next, κ is assumed to be a function of space. Cost functions and κ from such local DCF are shown in Fig. 4. As shown, further reduction of the cost function is obtained by assuming local κ as compared to the

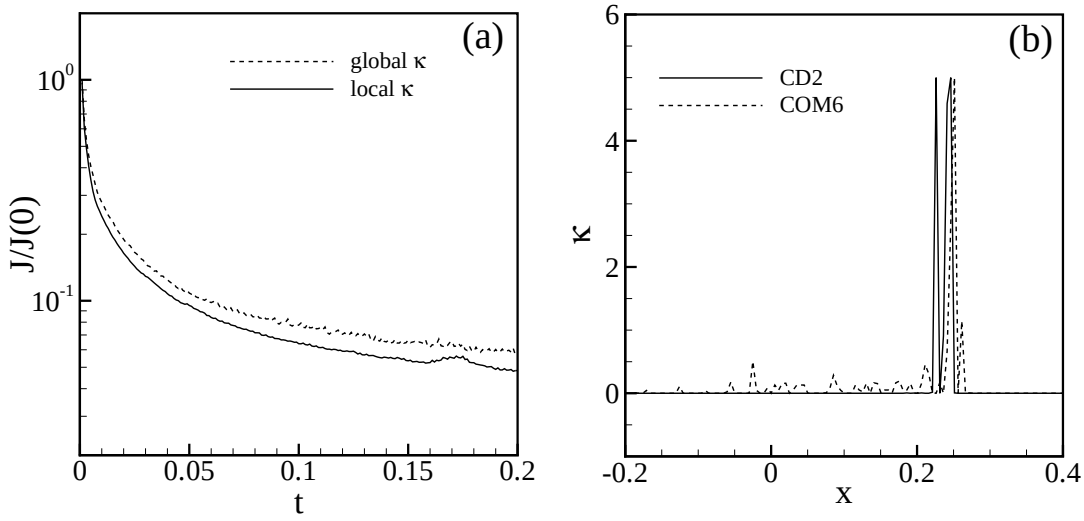

Figure 4. Cost functions and κ from the local dynamic model: (a) temporal evolutions of the cost functions from simulations with CD2, (b) instantaneous κ at $t = 0.14$ with CD2 and COM6 as base discretization schemes.

global DCF. It is also confirmed from Fig. 4 that such κ is highly localized in the vicinity of the shock. The performance of the local DCF is remarkable as shown in Fig. 5. It is especially true for the solutions with COM6 in which no wiggle is observed.

However, the computational cost of DCF is highly expensive when κ is local. In order to reduce the computational cost, we replaced the cost function (6) with a local cost function

$$\mathcal{J}_{local} = \theta_D \cdot IS(q) + \alpha\kappa^2 \tag{12}$$

based on the fact that the impact of changing κ should be local in space. Now, local κ is chosen at each grid point to minimize the local cost function (12). As shown in Fig. 6 for the same Sod problem, the local cost function is as effective as the global one. Thus, in what follows, all results are shown only from the local cost function.

Next, in order to evaluate the effect of the price term and discretization scheme, the shock-entropy interaction problem[9] is considered. Total grid point is $N = 200$ and the exact solution is obtained from $N = 3200$ simulation. As shown in Fig. 7, unlike the Sod problem, the solution is highly dependent upon the resolution property of the discretization scheme. It appears that the best solution is obtained with 6th order compact difference with a larger value ($\alpha = 0.03$) of the price term coefficient. Whereas, it is impossible to represent high-wavenumber oscillation in the region $1 < x < 2$ with CD2 without causing overall oscillation of the solution as shown in Fig. 7 (b).

Finally, the global DCF is applied to a two–dimensional mixing layer at vorticity thickness Reynolds number $Re_\delta = 1000$ and convective Mach number $M_c = 0.8$, as considered in Yee *et al.*[10] A coarse resolution of 81×81 is selected to highlight the performance of the shock capturing scheme. As shown in Fig. 8, κ increases in time as the vortex is rolling up and the shocklet is formed. Fig. 9 compares the temporal evolution of the temperature contours from DCF and the fixed κ simulation with $\kappa = 1$. It is clear that the proposed DCF outperforms the fixed κ simulation. At $T = 80$, contours from the fixed κ simulation shows smeared shock, which implies that $\kappa = 1$ is too high at this stage. Whereas, at $T = 160$ there are some wiggles near the shock, which implies κ should be higher to reduce the oscillation. In contrast to this, all results from DCF show clear capturing of shock without oscillation as well as vortical structures. Fig. 10 shows the local distribution of the instantaneous dynamic κ, which clearly shows that shock-capturing is highly localized only in the vicinity of the shock.

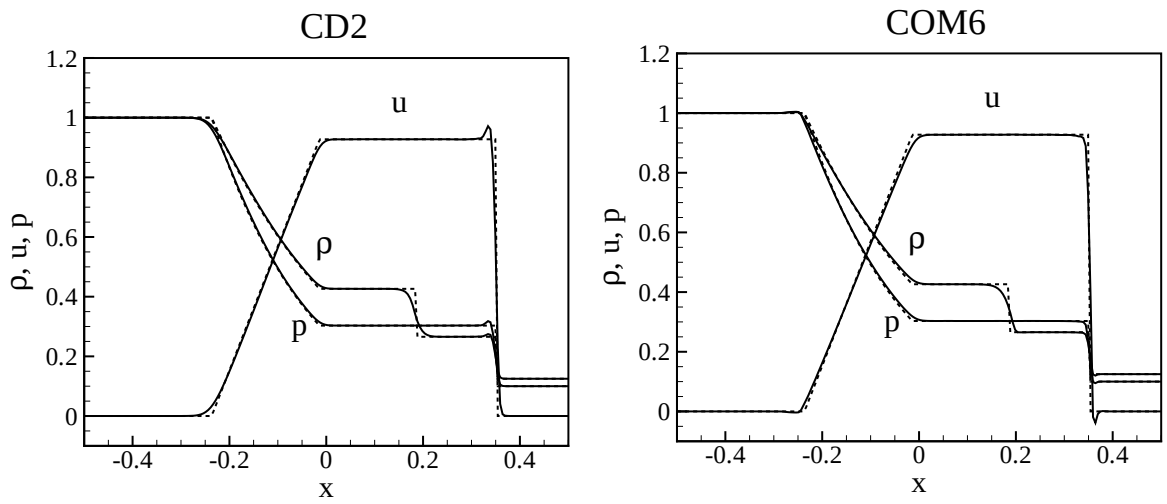

Figure 5. Solutions of the Sod problem at $t = 0.2$ from the local dynamic model. Solid lines are numerical solutions and dotted lines denote the exact Riemann solution.

V. Conclusion

In the present study, an efficient, suboptimal control–based dynamic procedure is proposed to determine the optimal coefficient for the filter numerical flux. The shock capturing problem is viewed as having three components, or 1) a good base shock capturing scheme, 2) the derivation of a good cost function with excellent localization property, and 3) efficient control algorithm. Note that the proposed method can be applied to any shock capturing schemes which can be incorporated in a time splitting manner.

Acknowledgments

This work was supported by the Office of Naval Research under grant N00014–08–1–0433. Computer time was provided by the Minnesota Supercomputing Institute, the San Diego Supercomputer Center, and the National Center for Supercomputing Applications.

References

[1]T. R. Bewley, P. Moin, and R. Temam, DNS-based predictive control of turbulence: an optimal benchmark for feedback algorithms, *J. Fluid Mech.* **447**, 119 (2001).

[2]F. Ducros, V. Ferrand, F. Nicoud, C. Weber, D. Darracq, C. Gacherieu and T. Poinsot, Large-eddy simulation of the shock/turbulence interaction, *J. Comput. Phys.* **152**, 517 (1999).

[3]S. Ghosh and K. Mahesh, Numerical simulation of the fluid dynamic effects of laser energy deposition in air, *J. Fluid Mech.*, **605**, 329 (2008)

[4]G. Jiang and C.-W. Shu, Efficient implementation of weighted ENO schemes, *J. Comput. Phys.* **126**, 202 (1996).

[5]F. Nicoud, J. S. Baggett, P. Moin, and W. Cabot, Large eddy simulation wall–modeling based on suboptimal control theory and linear stochastic estimation, *Phys. Fluids* **13**, 2970 (2001).

[6]N. Park and K. Mahesh, Numerical and modeling issues in LES of compressible turbulence on unstructured grids, *AIAA 2007-722* (2007).

[7]N. Park and K. Mahesh, Reduction of the Germano identity error in the dynamic Smagorinsky model, submitted to *Phys. Fluids* (2009)

[8]W. H. Press, B. P. Flannery, S. A. Teukolsky, and W. T. Vettering, *Numerical Recipes*, (Cambridge University Press, London 1986).

[9]C. W. Shu and S. Osher, Efficient implementation of essentially non-oscillatory shock-captuting schemes II, *J. Comput. Phys.* **83**, 32 (1989).

[10]H. C. Yee, N. D. Sandham and M. J. Djomehri, 1999, Low-dissipative high-order shock-capturing methods using characteristic-based filters, *J. Comput. Phys.* **150**: 199.

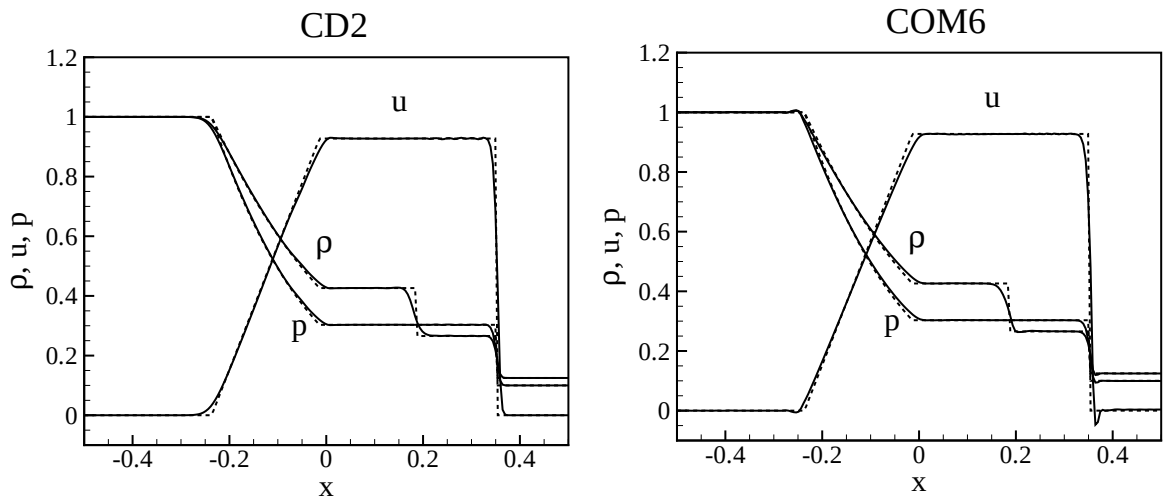

Figure 6. Solutions of the Sod problem at $t = 0.2$ from the local dynamic model with the local cost function. Solid lines are numerical solutions and dotted lines denote the exact Riemann solution.

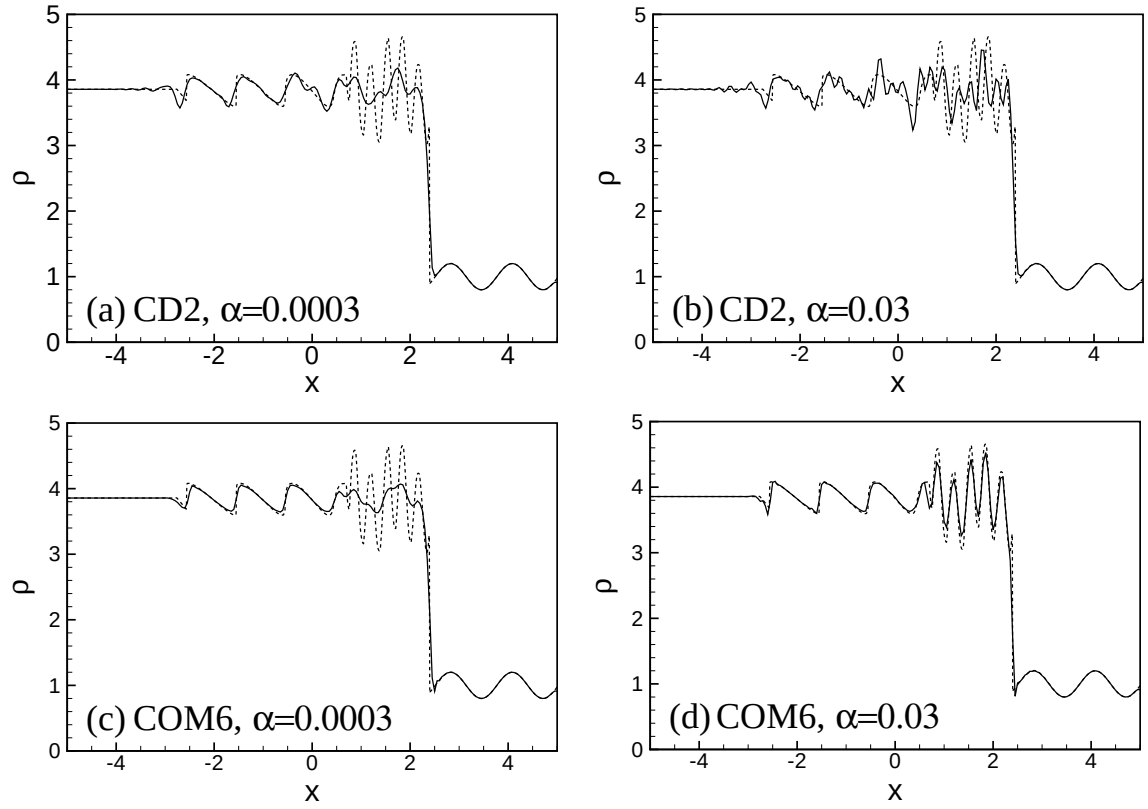

Figure 7. Solutions of the shock-entropy interaction at $t = 1.8$ from the local dynamic model. Solid lines are numerical solutions and dotted lines denote the exact solution.

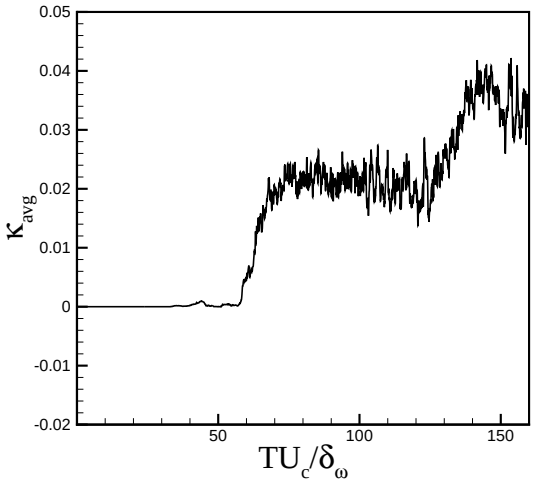

Figure 8. Temporal evolution of volume-averaged κ for yhe global dynamic model applied to a two–dimensional mixing layer at $Re_\delta = 1000$, $M_c = 0.8$ and 81×81 resolution.

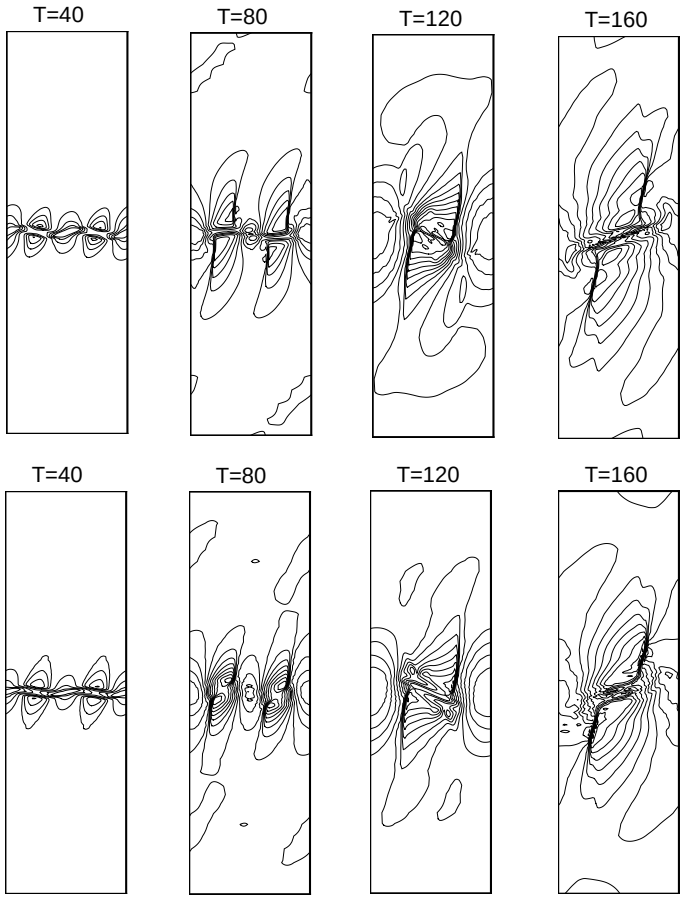

Figure 9. Temporal evolution of temperature contours of time-developing mixing layer from dynamic characteristic filter (upper row) and fixed $\kappa = 1$ (lower row).

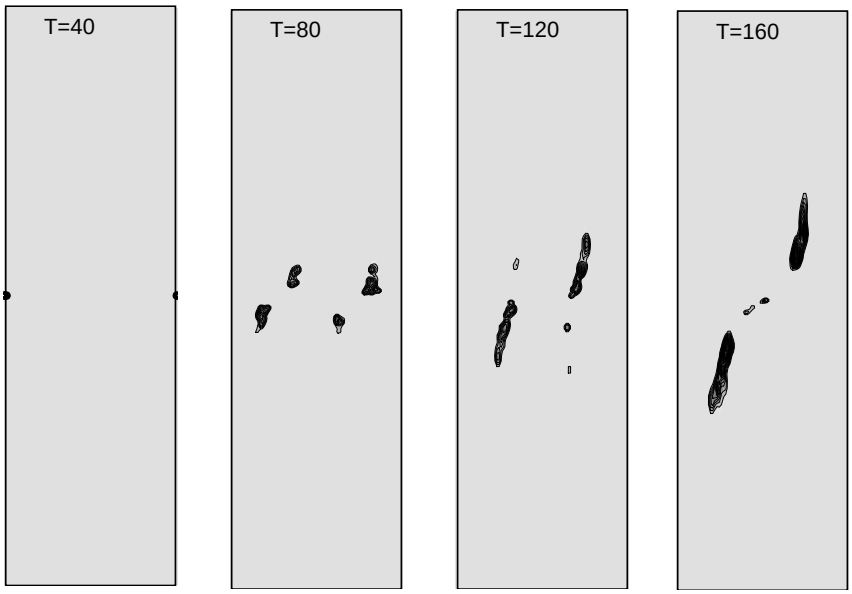

Figure 10. Temporal evolution of local dynamic κ for temporally developing mixing layer. Shown are 15 contours from $\kappa = 0.5$ to 5.